AD-776 956

A STUDY OF THE DIFFUSION ZONE BETWEEN Ta-10W TANTALUM ALLOY AND 4150 STEEL

Robert C. Tooke, et al

Rock Island Arsenal
Rock Island, Illinois

October 1973

R-RR-T-1-76-73

AD

A STUDY OF THE DIFFUSION ZONE BETWEEN Ta-10W TANTALUM ALLOY AND 4150 STEEL

TECHNICAL REPORT

Robert C. Tooke

and

Joseph D. DiBenedetto

October 1973

RESEARCH DIRECTORATE

GENERAL THOMAS J. RODMAN LABORATORY

ROCK ISLAND ARSENAL

ROCK ISLAND, ILLINOIS

UNCLASSIFIED

SECURITY CLASSIFICATION OF THIS PAGE (When Data Entered)

AD-776 956

REPORT DOCUMENTATION PAGE

READ INSTRUCTIONS BEFORE COMPLETING FORM

1. REPORT NUMBER: R-RR-T-1-76-73	2. GOVT ACCESSION NO.
3. RECIPIENT'S CATALOG NUMBER: b	
4. TITLE (and Subtitle): A STUDY OF THE DIFFUSION ZONE BETWEEN Ta-10W TANTALUM ALLOY AND 4150 STEEL	5. TYPE OF REPORT & PERIOD COVERED: Technical Report
6. PERFORMING ORG. REPORT NUMBER: R-RR-T-1-76-73	
7. AUTHOR(s): Robert C. Tooke and Joseph D. DiBenedetto	8. CONTRACT OR GRANT NUMBER(s)
9. PERFORMING ORGANIZATION NAME AND ADDRESS: CMDR, Rock Island Arsenal, GEN Thomas J. Rodman Laboratory, Rock Island, Illinois 61201	10. PROGRAM ELEMENT, PROJECT, TASK AREA & WORK UNIT NUMBERS: AMS Code 4930.16.6699
11. CONTROLLING OFFICE NAME AND ADDRESS: CMDR, Rock Island Arsenal, GEN Thomas J. Rodman Laboratory, Rock Island, Illinois 61201	12. REPORT DATE: October 1973
	13. NUMBER OF PAGES: 41
14. MONITORING AGENCY NAME & ADDRESS (if different from Controlling Office)	15. SECURITY CLASS. (of this report): UNCLASSIFIED
	15a. DECLASSIFICATION/DOWNGRADING SCHEDULE

16. DISTRIBUTION STATEMENT (of this Report)

Approved for public release, distribution unlimited.

17. DISTRIBUTION STATEMENT (of the abstract entered in Block 20, if different from Report)

18. SUPPLEMENTARY NOTES

19. KEY WORDS (Continue on reverse side if necessary and identify by block number)

1. Tantalum Alloy; 2. Refractory Alloy; 3. Steel; 4. Diffusion; 5. Tungsten Carbide; 6. Intermetallic; 7. Coextrusion

20. ABSTRACT (Continue on reverse side if necessary and identify by block number)

The formation and potential growth of an intermediate diffusion zone in coextruded gun barrels was investigated. Identification of the phases formed by diffusion between the tantalum alloy (Ta-10W) liner and the AISI 4150 steel jacket was accomplished by metallography, microhardness measurements, electron microprobe analysis, and X-ray diffraction. Isothermal treatments at 2000°F and 2400°F were performed to promote growth of the diffusion zone. A hard, brittle zone was formed as a result of diffusion, and the major phase constituent was determined to be tantalum carbide (TaC). Particles of the intermetallic Fe_2Ta

DD FORM 1 JAN 73 1473 EDITION OF 1 NOV 65 IS OBSOLETE

UNCLASSIFIED

SECURITY CLASSIFICATION OF THIS PAGE (When Data Entered)

20. and indications of a few tungsten-rich particles (probably tungsten carbides) were detected dispersed in the TaC. Carbon depletion of the steel adjacent to the interface occurred as a result of carbon diffusion into the tantalum alloy forming TaC. Tungsten was found to diffuse for considerable distances into the steel at both temperatures as contrasted to the tantalum which did not. When the diffusion zone was isothermally treated to sufficient thickness, the liner could be separated from the jacket when short longitudinal sections were stressed to cause fracture of the zone. However, the diffusion times and temperatures necessary to enlarge the diffusion zone to this critical thickness are not attainable in gun barrel environments. (U) (Tooke, R. C. and DiBenedetto, J. D.)

CONTENTS

INTRODUCTION

Because of the erosive conditions to which barrel materials are subjected during the rapid firing of guns, materials for barrels had to be improved. One such improvement involved the lining of the bore of an AISI 4150 steel barrel with a tantalum alloy (Ta-10W). The Ta-10W lined barrel was superior to the standard Cr plated barrel under comparative test firing. A Research Directorate, RIA report[1] documents the techniques used to manufacture the multilayer gun barrel, the results of firing tests, and metallurgical examinations. Only the information essential to establishing the relevancy of the present investigation to maintain continuity will be repeated.

The Ta-10W alloy liner and the 4150 steel were coextruded at 1900°F to form a multilayer gun tube. The extrusion produced a satisfactory bond, mechanical and metallurgical in nature, between the steel and refractory alloy liner. Metallurgical bonding was accomplished through an intermediate diffusion zone, and representative areas of the interface are depicted in Figure 1. Several of the lined tubes were cold-swaged to form rifled blanks for use as M134 Minigun barrels. The brittle characteristic of the diffusion zone is illustrated in Figure 2 which reveals the fragmenting that occurred in this zone during swaging.

Although detrimental effects during test firing cannot be attributed to the diffusion zone, this zone could be a potential trouble area. Consequently, information pertaining to the diffusion zone was desirable.

PROCEDURE

Sections of a coextruded gun tube were used to analyze the diffusion zone between the 4150 steel and the Ta-10W liner. The diffusion zone in the as-extruded condition was not of sufficient dimensions to permit thorough compositional analysis; therefore, a series of isothermal treatments at elevated temperature were performed to facilitate growth of the interfacial zone by diffusion. Specimens subjected to isothermal treatments were prepared by removal of excess steel stock from the gun tube resulting in a specimen 0.6 inch in diameter and cut to 1 inch in length. All isothermal treatments were conducted in a Leco Glo-Bar furnace adapted for argon atmosphere operation. Observation of the specimens after removal from the furnace showed no oxidation, which indicated that the inert gas protection was satisfactory. Identification of the specimens used in this study is presented in Table I.

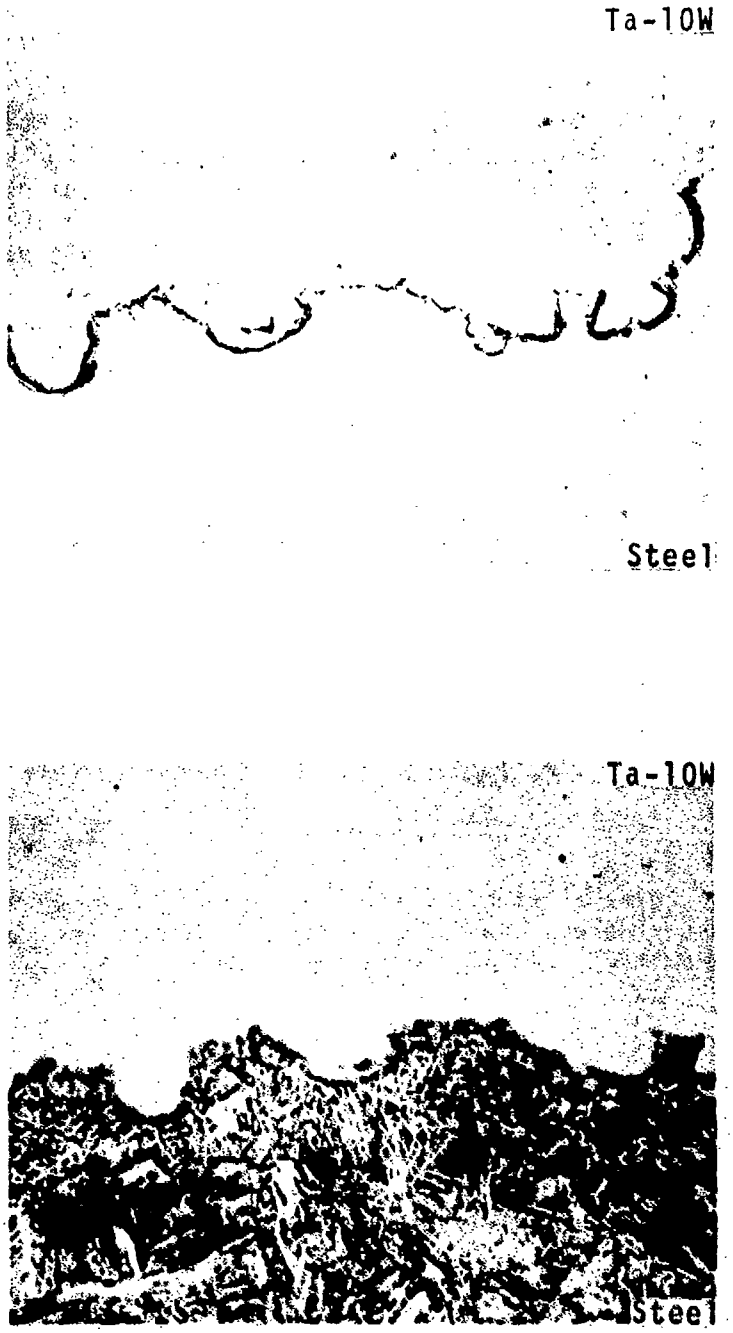

FIGURE 1 Interface between 4150 Steel and Ta-10W Alloy at 750X. Note Diffusion Zone in Unetched (top) and Nital Etched (bottom) Conditions

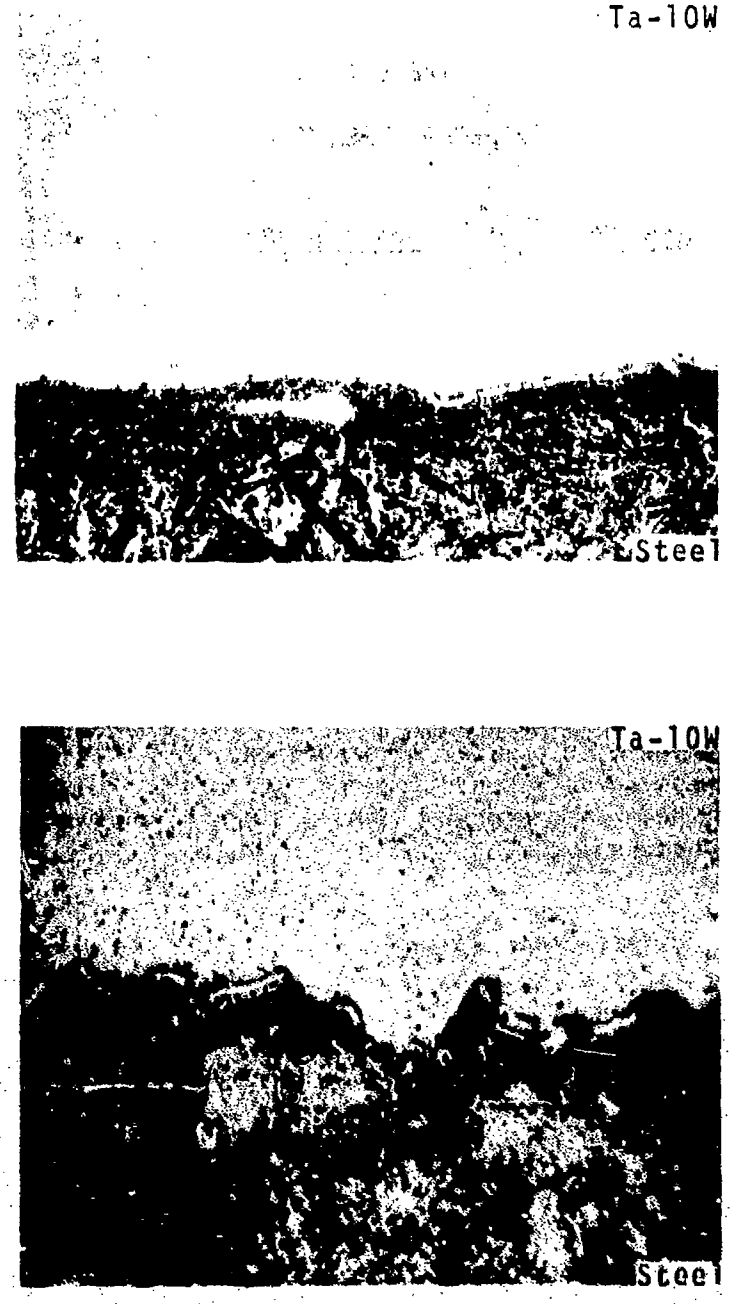

FIGURE 2 Longitudinal (top) and Transverse (bottom) Sections showing Fragmentation of Diffusion Zone after Cold Swaging. Nital Etch, 750X

TABLE I

ISOTHERMAL TREATMENTS

Specimen	Description
0	as extruded
1	1 hour at 2000°F
2	2 hours at 2000°F
3	3 hours at 2000°F
4	15.5 hours at 2000°F
5	24 hours at 2400°F

Several techniques were used to analyze the diffusion zone. These techniques included optical metallography, X-ray diffraction, Tukon microhardness surveys, and electron microprobe analysis. Specific procedural details concerning analysis of the diffusion zone will be described as necessary.

Considerable difficulty was encountered in the metallographic preparation of specimens which contained the steel, the tantalum alloy, and the intermediate compounds in the diffusion zone. Differences in hardness required the use of procedures which minimized surface relief, namely, polishing primarily with diamond abrasive on nylon cloths. Only light lapping with alumina could be used. Also, metallographic preparation of the Ta-10W alloy[2,3] requires chemical etching with reagents which rapidly dissolve the steel. The procedures used in the preparation of specimens for metallographic analysis are a compromise since a high quality polished and etched surface in the steel, diffusion zone, and Ta-10W alloy was impossible to obtain simultaneously.

RESULTS

The growth of the diffusion zone, as a result of the various isothermal treatments, can be observed by the series of microstructures presented in Figures 3 through 8. Specimens for metallographic analysis were prepared so that the optimum polish and etch existed in the vicinity of the diffusion zone. The steel has been etched, but the Ta-10W by necessity remains in the unetched condition.

FIGURE 3 Specimen No. 0 - Original As Extruded Condition. Transverse Section, 400X, Nital Etch

FIGURE 4 Specimen No. 1 - 1 Hour at 2000°F. Transverse Section, 400X, Nital Etch

FIGURE 5 Specimen No. 2 - 2 Hours at 2000°F. Transverse Section, 400X, Nital Etch

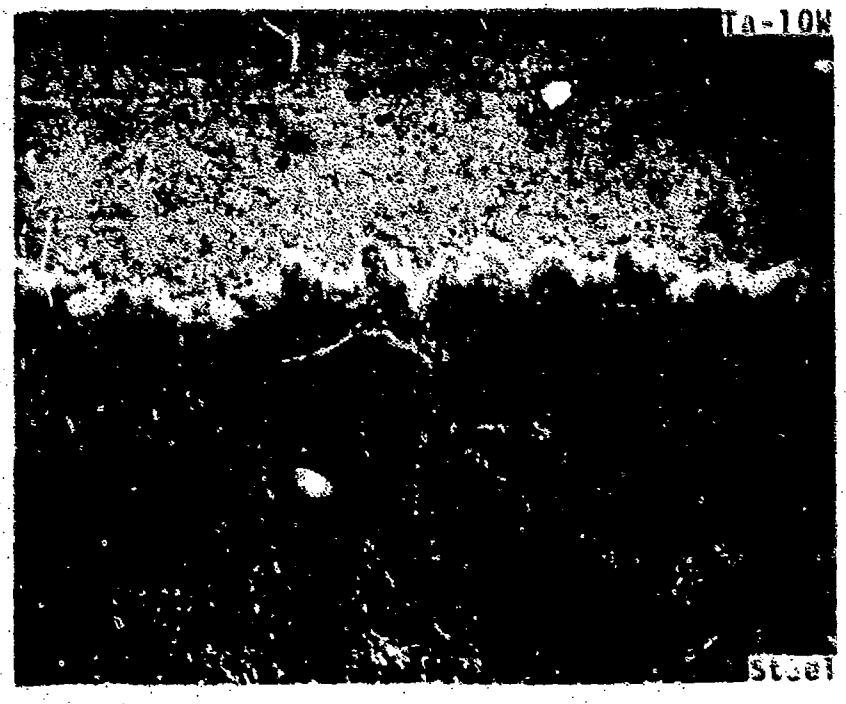

FIGURE 6 Specimen No. 3 - 3 Hours at 2000°F. Transverse Section, 400X, Nital Etch

FIGURE 7 Specimen No. 4 - 15.5 Hours at 2000°F. Transverse Section, 400X, Nital Etch

FIGURE 8 Same as Figure 7 Except at 800X. Note the Change in Structure on the Steel Side of the Diffusion Zone

The most visible part of the diffusion zone appears white in these microstructures; however, other changes in the microstructure have occurred as evidenced in Figure 8. The same type of microstructure on the steel side of the interface can be seen by close observation of previous samples. This zone in the steel appears to be lower in carbon than the steel matrix.

The growth of the white zone is primarily in the direction of the Ta-10W alloy and is verified by the smooth Ta-10W white zone boundary as diffusion proceeds. Measurements of the width of the white zone were taken, and the results show a parabolic growth of this zone with time as described by the equation:

$W = \sqrt{Kt}$

W = width of white zone (in.)

K = growth rate constant ($in.^2/min.$)

t = time (min.)

The data for Specimens 1 through 4 are contained in Table II and are presented graphically in Figure 9. The graph plotted in Figure 9 is for $K = 4.4 \times 10^{-10}$ $in.^2/min.$

TABLE II

MEASUREMENTS OF WHITE ZONE
AND CALCULATED GROWTH RATE CONSTANT

Specimen	Width of White Zone W (Inches)	Growth Rate Constant K ($inches^2$/minute)
0	1.00×10^{-4}	----------
1	1.53×10^{-4}	3.92×10^{-10}
2	2.23×10^{-4}	4.15×10^{-10}
3	2.95×10^{-4}	4.84×10^{-10}
4	6.69×10^{-4}	4.80×10^{-10}

Specimen 5, heated at 2400°F for 24 hours, is the most useful sample for analytical purposes and has been analyzed more completely than the others. The results of sequential etching of this sample are shown in Figures 10 through 17.

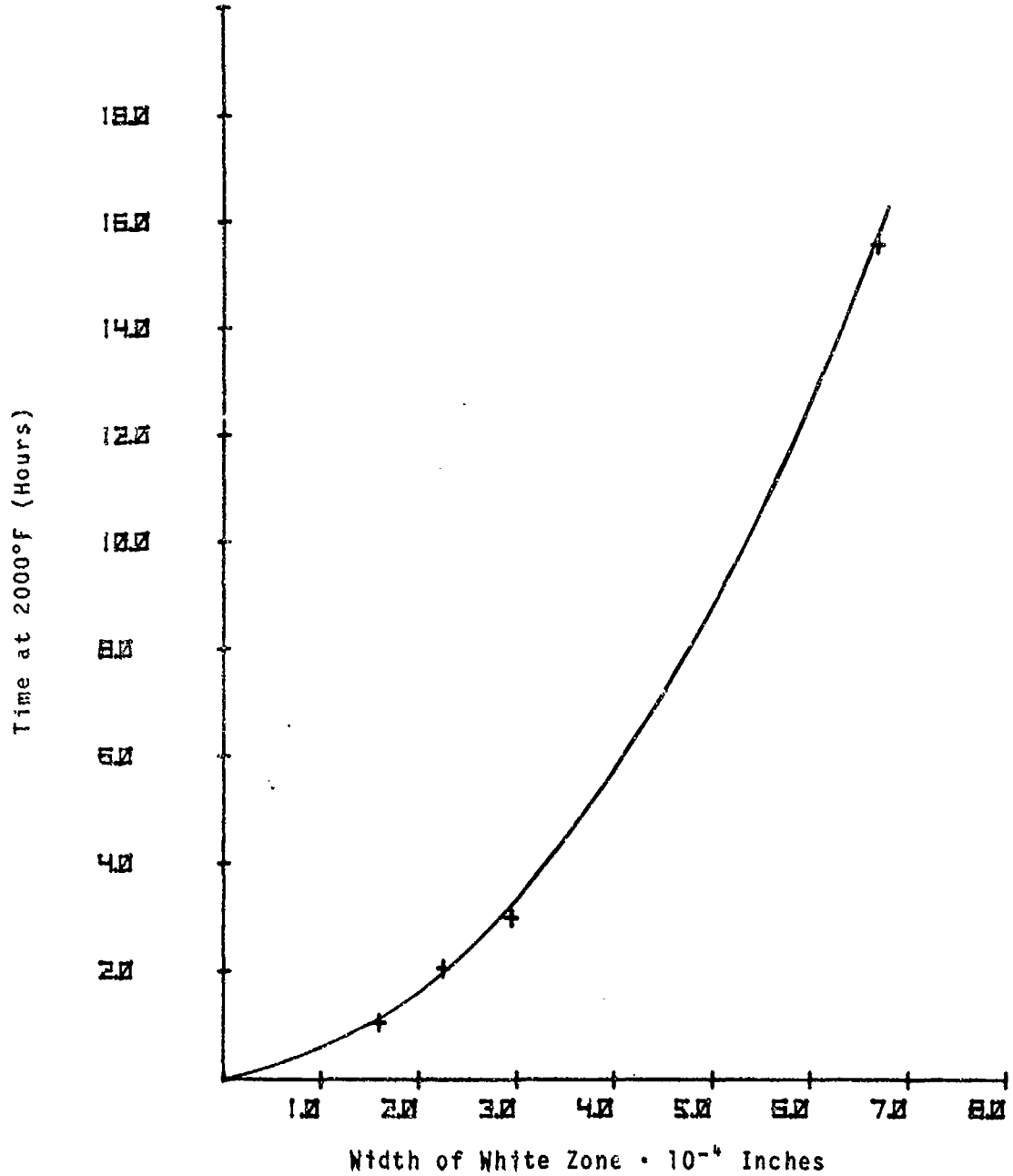

FIGURE 9 Growth of White Zone at Ta-10W Steel Interface

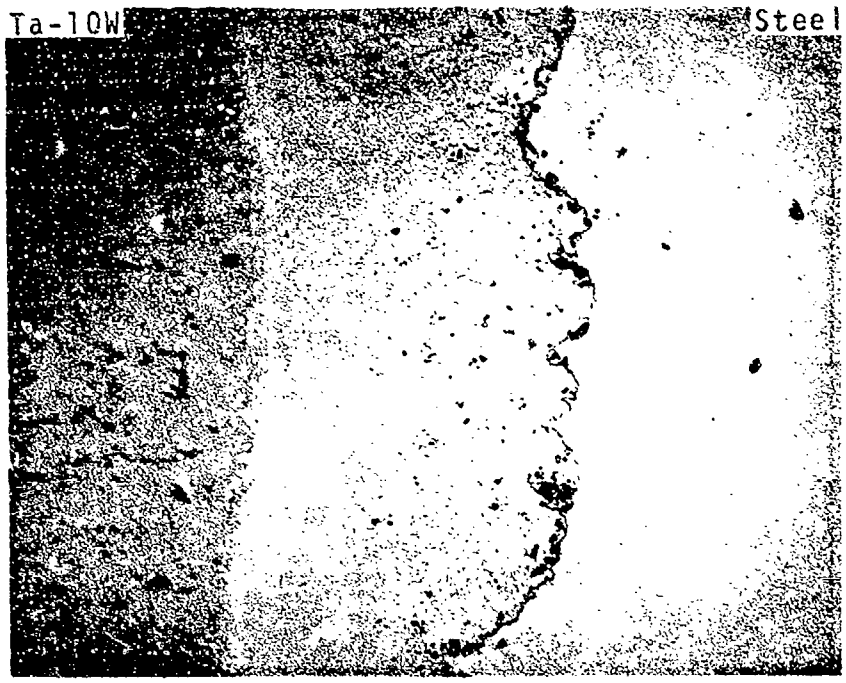

FIGURE 10 Transverse Section of Specimen No. 5, Unetched at 400X

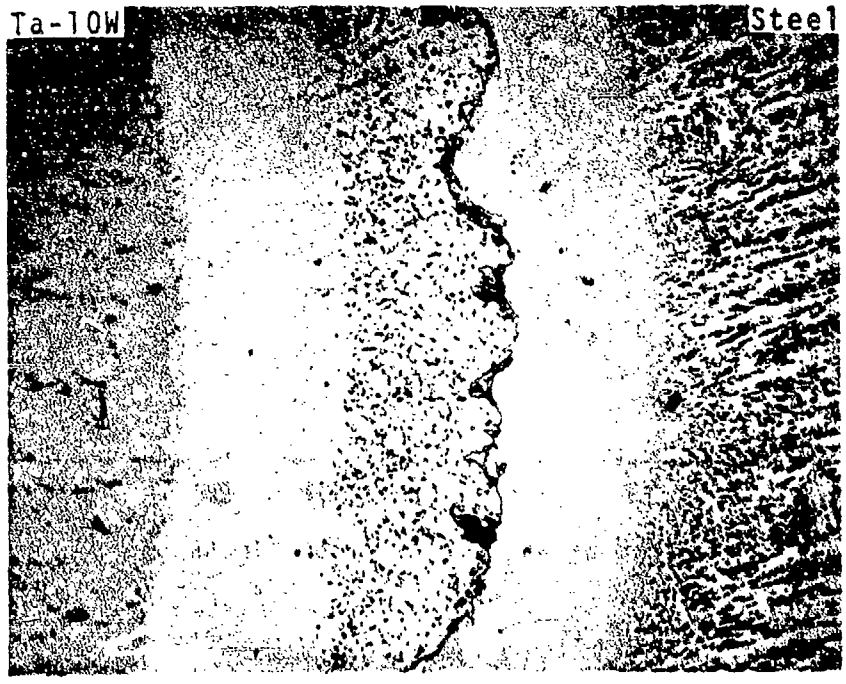

FIGURE 11 Specimen No. 5, 400X, Etched 6 sec. in 2% Nital. Note the Appearance of New Part of Diffusion Zone on the Steel Side which is Resistant to Nital Etch

FIGURE 12 Specimen No. 5, 400X, Etched 12 sec. in 2% Nital. Further Etching has Revealed Microstructure of Region Adjacent to Steel

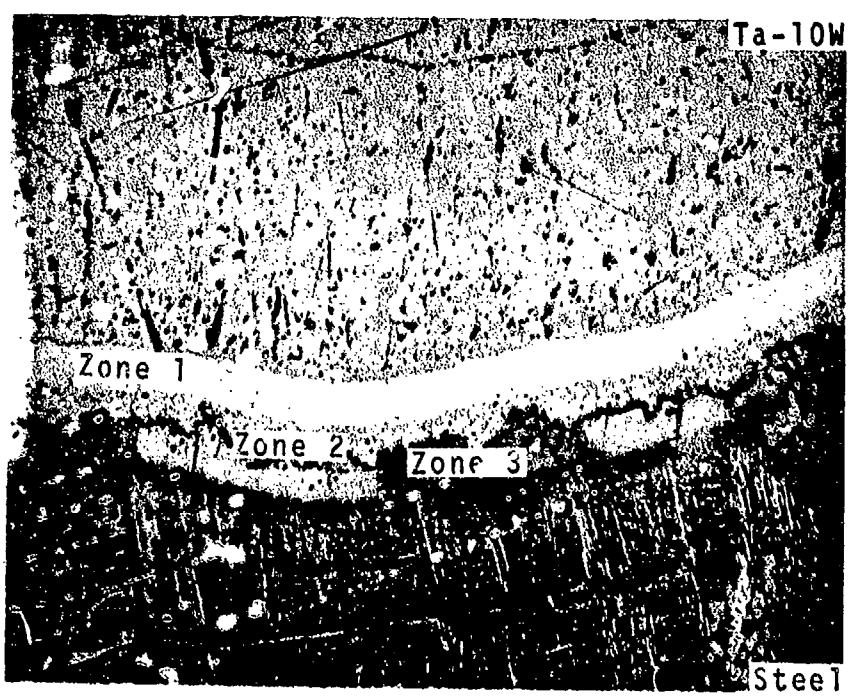

FIGURE 13 Same as Figure 12 Except at 100X. The Intermediate Zones Shown have a Combined Width of .007"

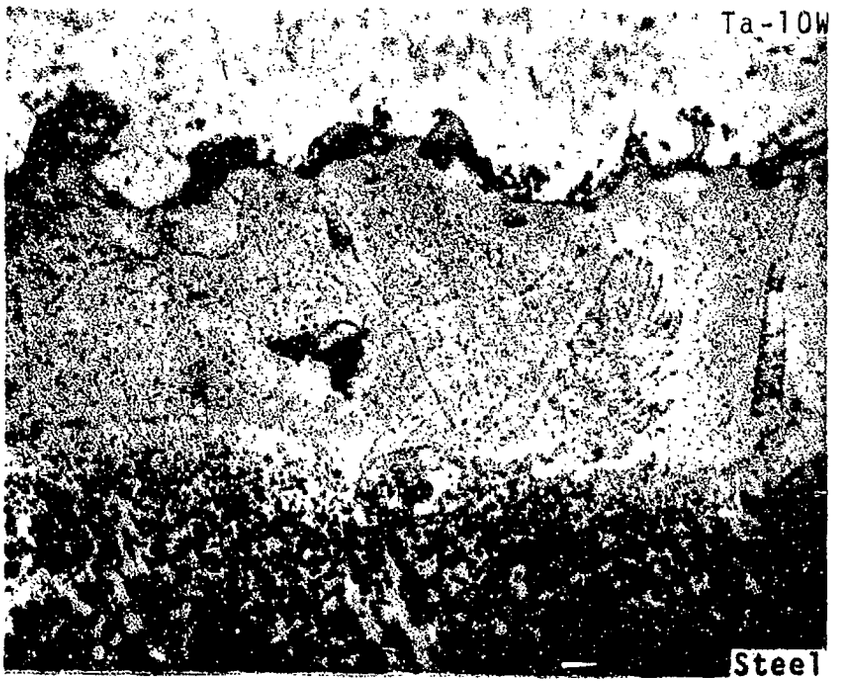

FIGURE 14 Specimen No. 5 Etched 12 sec. in 2% Nital. Observe the Precipitate, in the Zone Adjacent to the Steel, which has been Resolved at 800X

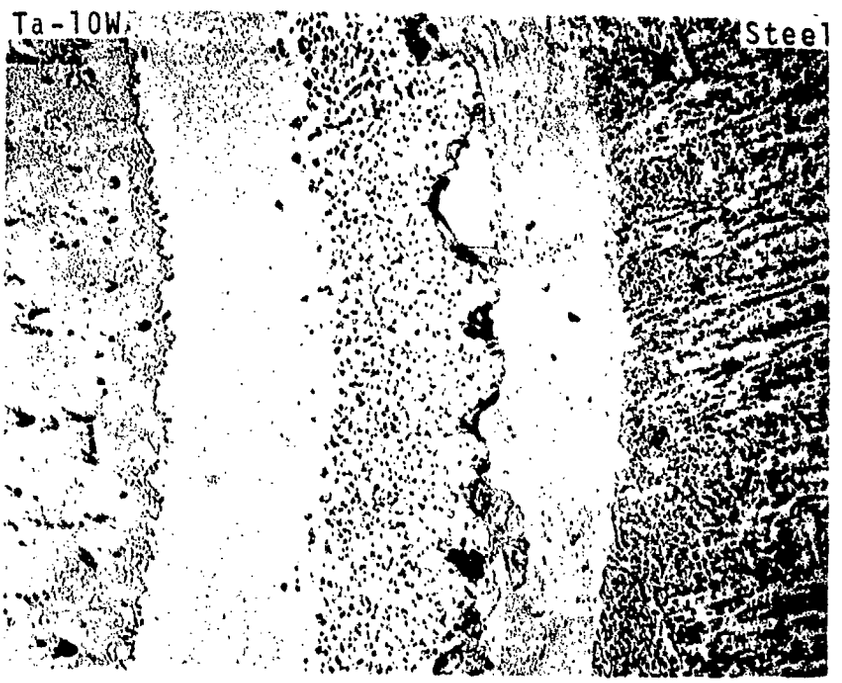

FIGURE 15 Specimen No. 5, 400X, Swabbed with 48% HF Following Nital Etch to Show the Diffuse Boundary Between Ta-10W and the Diffusion Zone

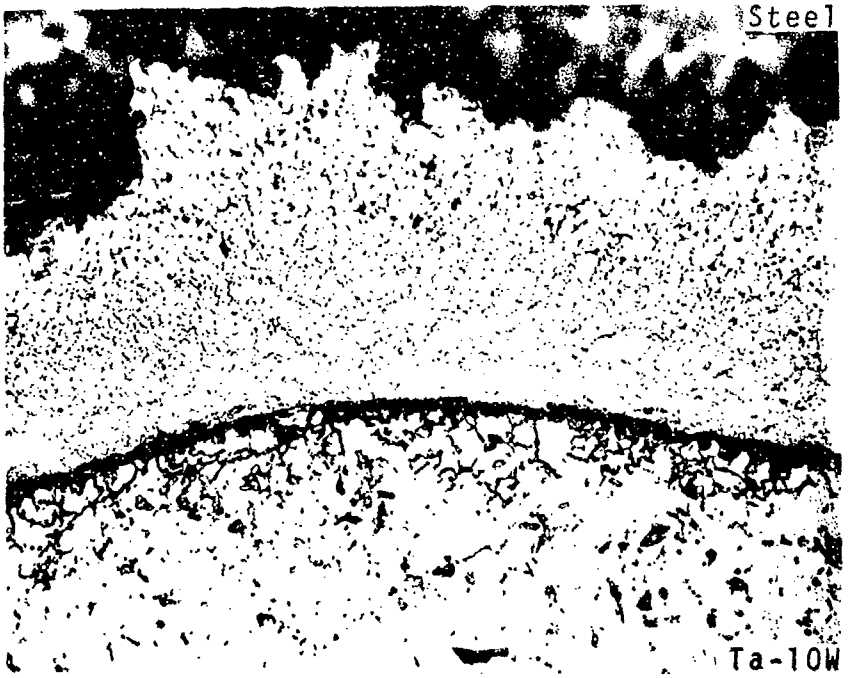

FIGURE 16 Specimen No. 5, 400X, after Swabbing with and by Immersion in Lactic, Nitric, and Hydrofluoric Acid Etchant which Chemically Polishes the Ta Alloy and Dissolves the Steel

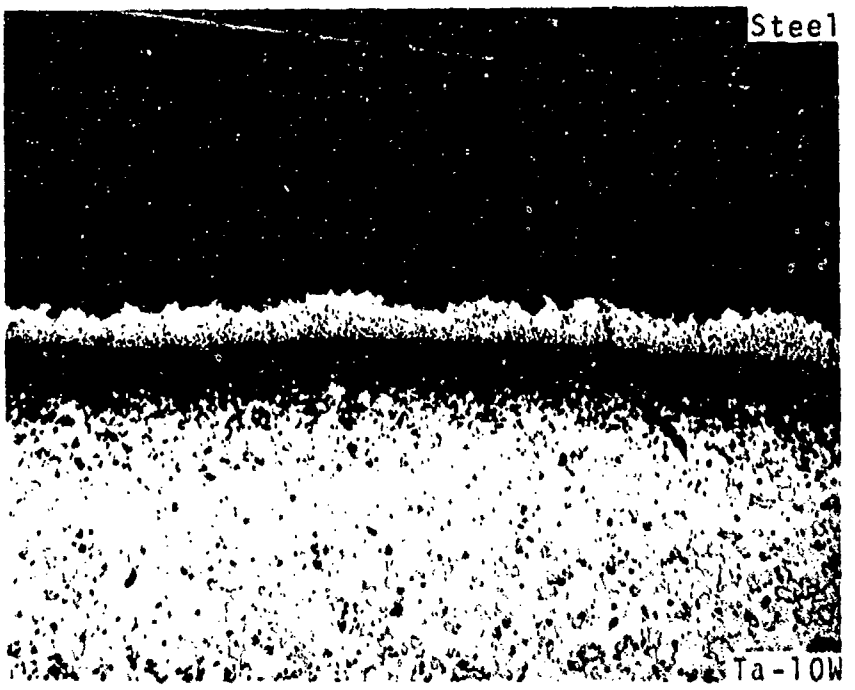

FIGURE 17 Specimen No. 5, 100X, after Further Chemical Polishing of the Ta-10W and Etching by Immersion in a 20% Solution of Ammonium Bifluoride to Reveal the Latent Grain Boundaries in Ta-10W Alloy

The microstructures show three distinct zones (Figure 13) in the region formed by diffusion. The ragged boundary between Zones 2 and 3 is comparable to the original interface between the steel and the Ta-10W alloy. However, the movement of this interface is possibly due to differences in diffusion rates and volume changes resulting from the formation of new phases.

Etching behavior reveals Zone 3 is an iron-rich zone, low in carbon, similar to the one shown previously in Figure 8. The white zone extends through Zones 1 and 2. Justification for the preceding statement is the absence of a distinct boundary between Zones 1 and 2. The white zone forms the matrix for Zone 2, with particles of other phases dispersed throughout this zone. The etching characteristics of the materials, illustrated in Figures 16 and 17, seem to be a contradiction of the above conclusion since Zone 1 is attacked much more rapidly than Zone 2. However, subsequent results and discussion are provided that will explain this behavior and reinforce the conclusion that the white zone extends through Zones 1 and 2.

Tukon microhardness measurements, taken on Specimens 4 and 5, are shown in Figures 18 and 19, respectively. The white zone of Specimen 4 and Zones 1 and 2 of Specimen 5 were extremely hard. Zone 3 of Specimen 5 is comparably soft, as would be expected if this is a zone depleted in carbon. Specimen 4, however, shows a slight increase in hardness on the steel side of the white zone. This increase is attributed to the proximity of the hard white zone and is not considered representative of the structure.

Electron microprobe analysis provided the information contained in Figure 20 (Specimen 4) and Figure 21 (Specimen 5). These plots are the average of several strip chart recordings obtained while traversing the diffusion zone. No useful results were obtained from Specimen 10 since the diffusion zone did not have sufficient thickness.

Specimen 4 was reported to have a visible reaction zone of approximately two mils. The white zone of Specimen 4 (Table 1) was not this thick so apparently the specimen for microprobe analysis was not a true transverse section or perhaps the scan was not perpendicular to the interface. Whatever the reason, the linear dimensions along the abscissa of Figure 20 are not absolute, but they can be roughly normalized to a more agreeable value when multiplied by one-half. The white zone of Specimen 4 was a uniform-gradient diffusion area. Iron dropped immediately to approximately 8 to 10 weight per cent at the interface and decreased uniformly to 0 at the inner edge of the zone. Tantalum concentration dropped gradually through the diffusion zone

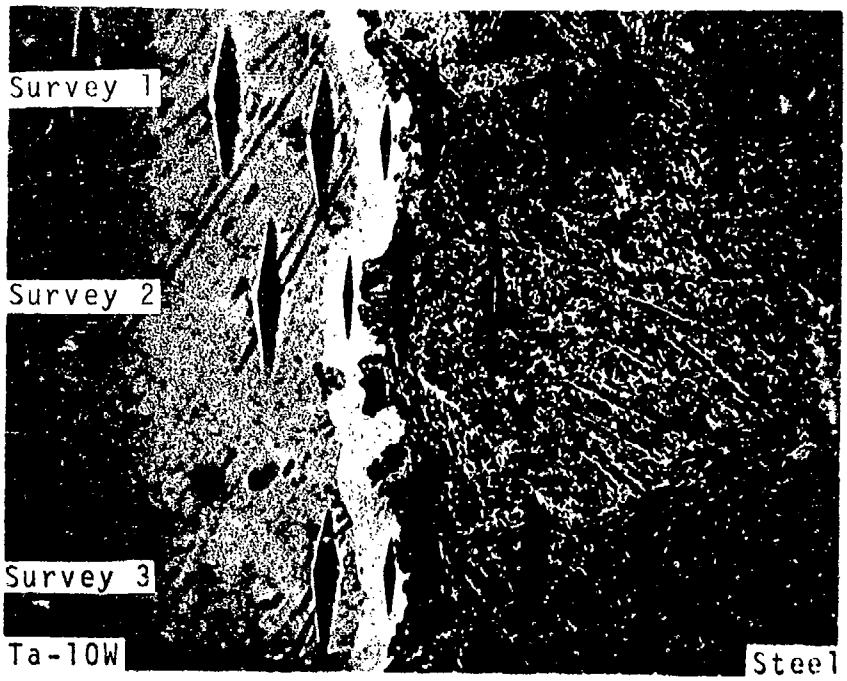

Survey	Position	Filar Units	Knoop Hardness Number (KHN)
1	Ta-10W	339	451
1	Ta-10W	312	532
1	Ta-10W	287	629
1	White zone	160	2034
1	Steel	321	505
1	Steel	372	374
1	Steel	386	348
2	Ta-10W	334	465
2	White zone	183	1590
2	Steel	346	433
2	Steel	360	400
3	Ta-10W	306	555
3	White zone	164	1936
3	Steel	321	505
3	Steel	360	400
3	Steel	359	402

FIGURE 18 Results of Tukon Microhardness Surveys (.1Kg load) on Specimen No. 4. Mag. 400X.

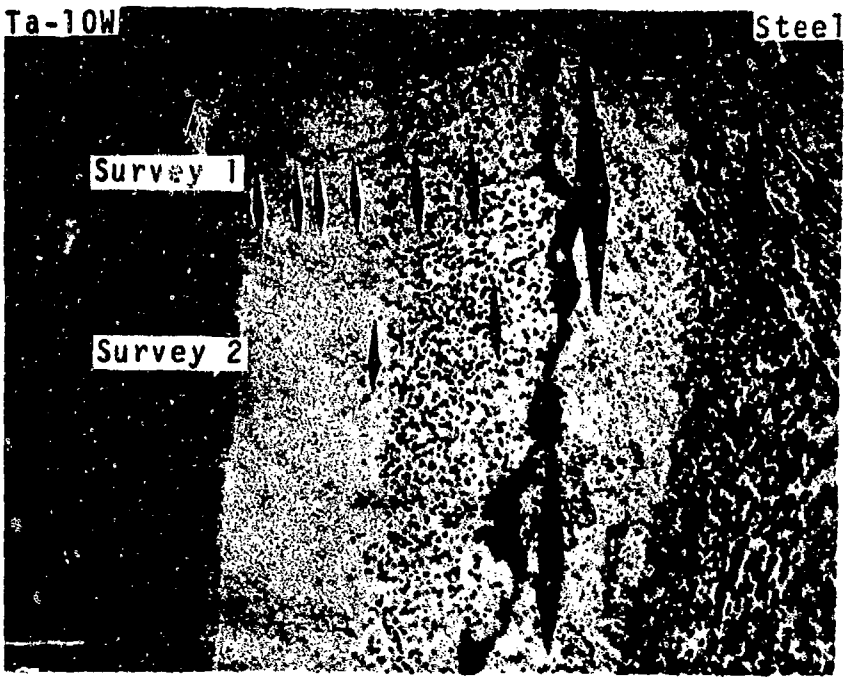

Survey	Position	Filar Units	Knoop Hardness Number (KHN)
1	Ta-10W	332	469
1	Zone 1	158	2086
1	Zone 1	150	2314
1	Zone 1	150	2314
1	Zone 1	154	2196
1	Zone 2	170	1802
1	Zone 2	169	1830
1	Zone 3	535	182
1	Steel	360	400
2	Zone 1 - Zone 2	160	2034
2	Zone 2	175	1700

FIGURE 19 Results of Tukon Microhardness Surveys (.1Kg load) on Specimen No. 5. Mag. 400X.

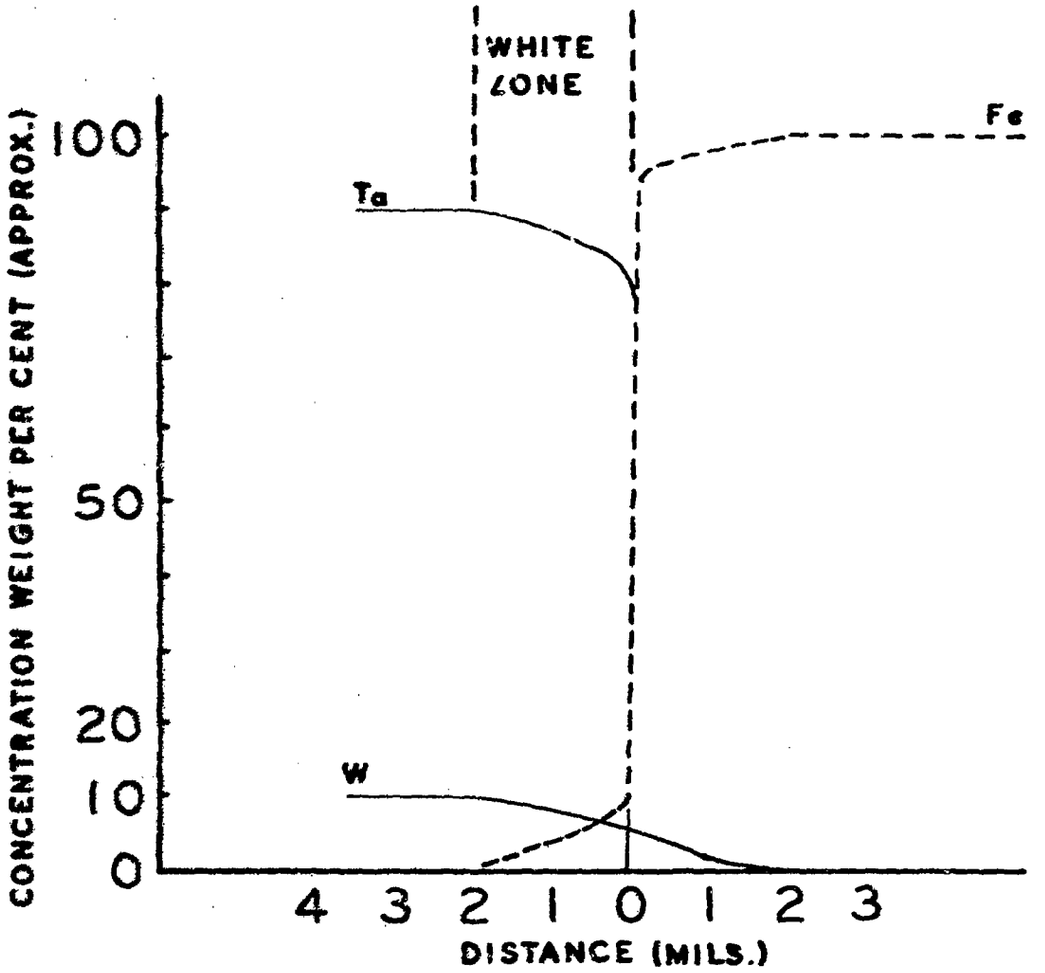

FIGURE 20 Electron Microprobe Analysis of Specimen No. 4

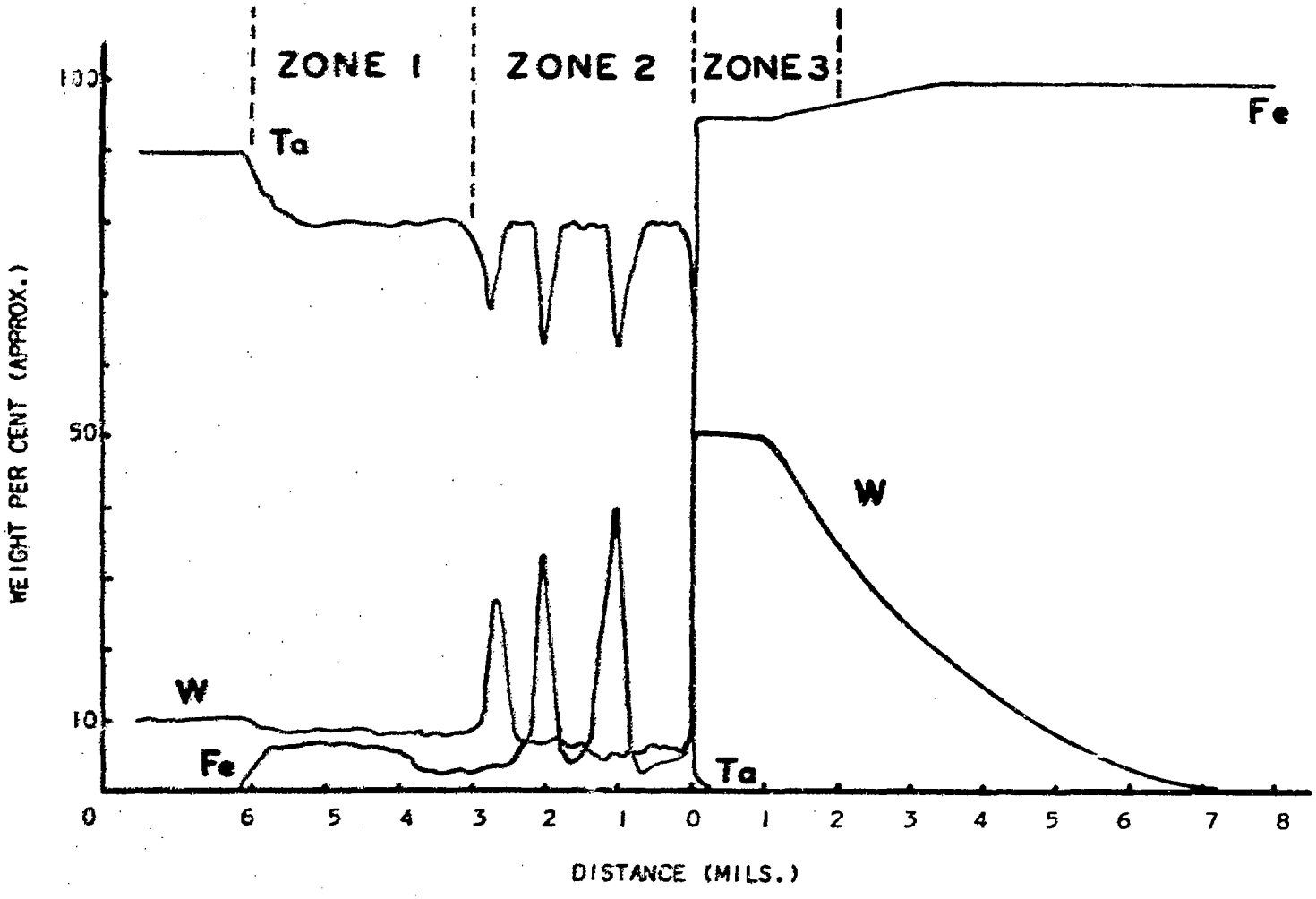

FIGURE 21 Electron Microprobe Analysis of Specimen No. 5

from the 90 weight per cent in the liner alloy to 80 weight per cent near the opposite edge of the white zone at which point it quickly decreased to 0. The concentration of the tungsten dropped from the alloy concentration to approximately 5 weight per cent at the steel - white zone boundary and then decreased to 0 within the steel.

In Specimen 5 (Figure 21), the tungsten has diffused for a much greater distance, as far as 7 mils from the original interface. Also, a zone of about 1 mil occurred where the tungsten concentration remained fairly constant at approximately 5 weight per cent. Particles, rich in iron, and a few tungsten-rich particles were found in Zone 2. The tantalum concentration remained constant (80 weight per cent) in Zones 1 and 2, except for dips associated with the iron and tungsten particles. The iron and especially the tungsten particle concentrations, as plotted, are estimated because the particle size and surface conditions precluded accurate analysis.

Numerous X-ray diffraction patterns were obtained by use of three techniques. Only the most conclusive patterns will be presented. However, X-ray analysis involved many other patterns which proved that the results are reproducible, but did not provide additional information. A summary of the results of X-ray diffraction is presented in Table III. Actual X-ray patterns are shown in Figures 22 through 30. The X-ray data used for analyzing the patterns are presented in Table IV which also includes a comparison of patterns G and H with these data. The source of this reference data is the ASTM card file, with the exception of the data for Fe_2Ta as reported by Wallbaum.[4] The Ta-10W alloy lattice parameter varied only slightly from that of tantalum which was used to identify the Ta-10W phase.

The X-ray data indicate an abundance of TaC in the diffusion zone. The white zone of Specimen 4 was identified as TaC. Analysis of Specimen 5 showed that TaC is present in contact with αFe and with Ta-10W which indicates TaC is the major phase in Zones 1 and 2. The intermetallic Fe_2Ta was detected somewhat sporadically, the low angle lines being the prime basis for identification. Pattern J, which strongly shows these low angle lines, gave some inference to the position of the intermetallic being below the TaC since the Fe_2Ta was not detected until some material was removed from the surface (compare patterns I and J).

DISCUSSION OF RESULTS

Examination of the data establishes TaC to be the primary product

TABLE III

SUMMARY OF X-RAY ANALYSIS

Pattern	Figure	Description	Technique	Phases Identified
A	22	Specimen 4, X-ray beam hitting convex surface of diffusion zone exposed after steel was dissolved in HCl.	Diffractometer (CuKα)	TaC
B	23	Specimen 5, longitudinal section polished at low angle to diffusion zone which widened the zone for exposure to the finely collimated beam.	Diffractometer (CuKα)	TaC
C	24	Same as pattern B except X-ray beam placement favored steel side of zone.	Diffractometer (CuKα)	TaC,αFe
D	25	Same as pattern B except X-ray beam placement favored Ta-10W side of zone.	Diffractometer (CuKα)	TaC,Ta-10W
E	26	Specimen 5 fractured circumferentially through the diffusion zone along the boundary between Zones 2 and 3. Liner side of fracture surface exposed to X-ray.	Diffractometer (CuKα)	TaC,αFe, Fe_2Ta
F	27	Same as pattern E except steel side of fracture surface exposed to X-ray.	Diffractometer (CuKα)	αFe,TaC,Fe_2Ta
G	28	Powder sample obtained by removing fine chips and slivers from diffusion zone fracture surface.	Debye Scherrer powder (CuKα)	TaC,Fe_2Ta, Ta-10W αFe
H	28	Same procedure as pattern G.	Debye Scherrer powder (CuKα)	TaC,Fe_2Ta, Ta-10W αFe
I	29	Specimen 5, liner side of fracture surface.	Glancing back reflection off stationary polycrystalline sample. $CuK\alpha_1$ (Si monochromator)	TaC,αFe
J	30	Same as pattern I except after some fragments were removed from fracture surface.	Glancing back reflection off stationary polycrystalline sample. $CuK\alpha_1$ (Si monochromator)	TaC,Fe_2Ta

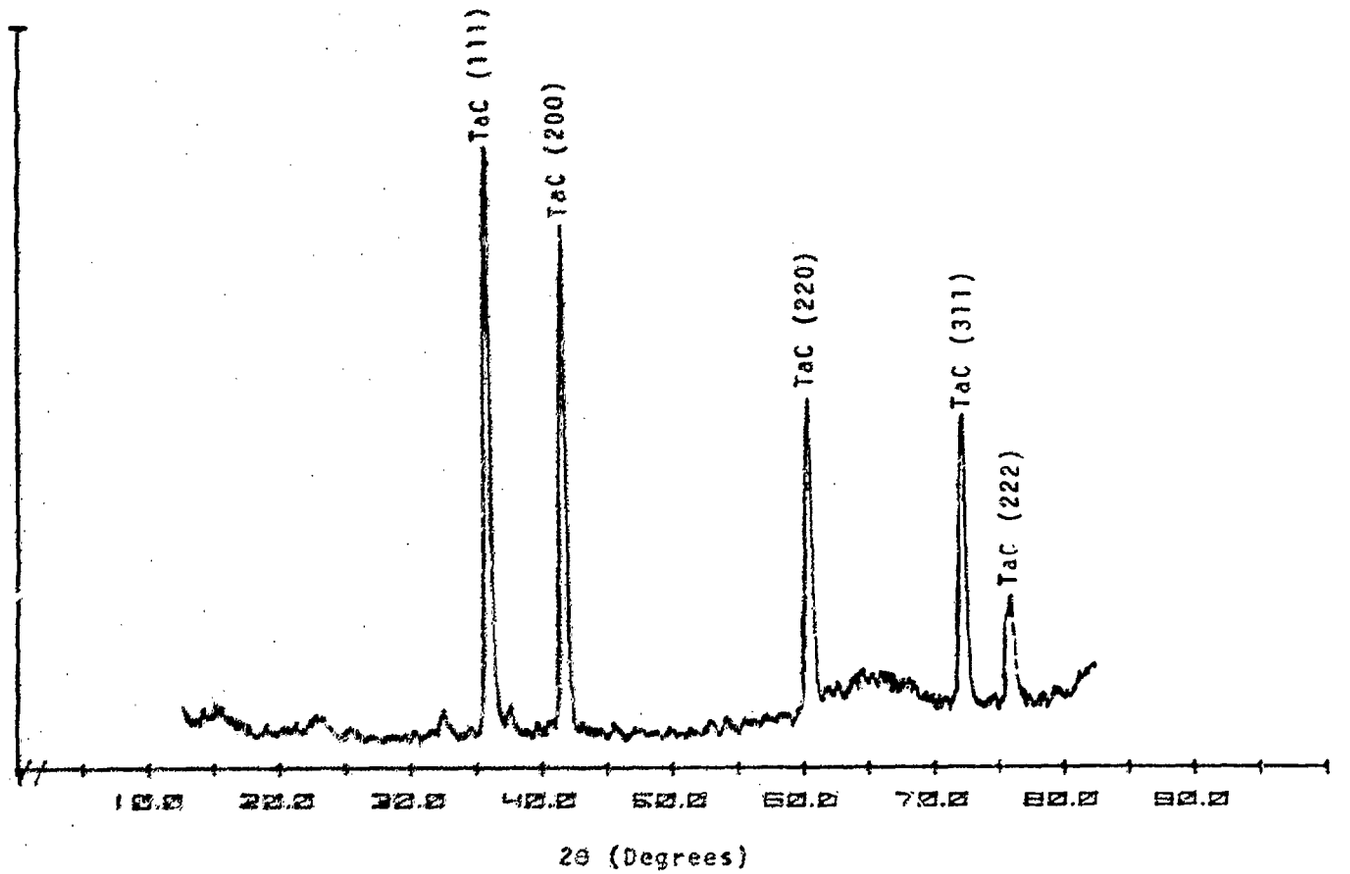

FIGURE 22. X-Ray Diffraction Pattern A.

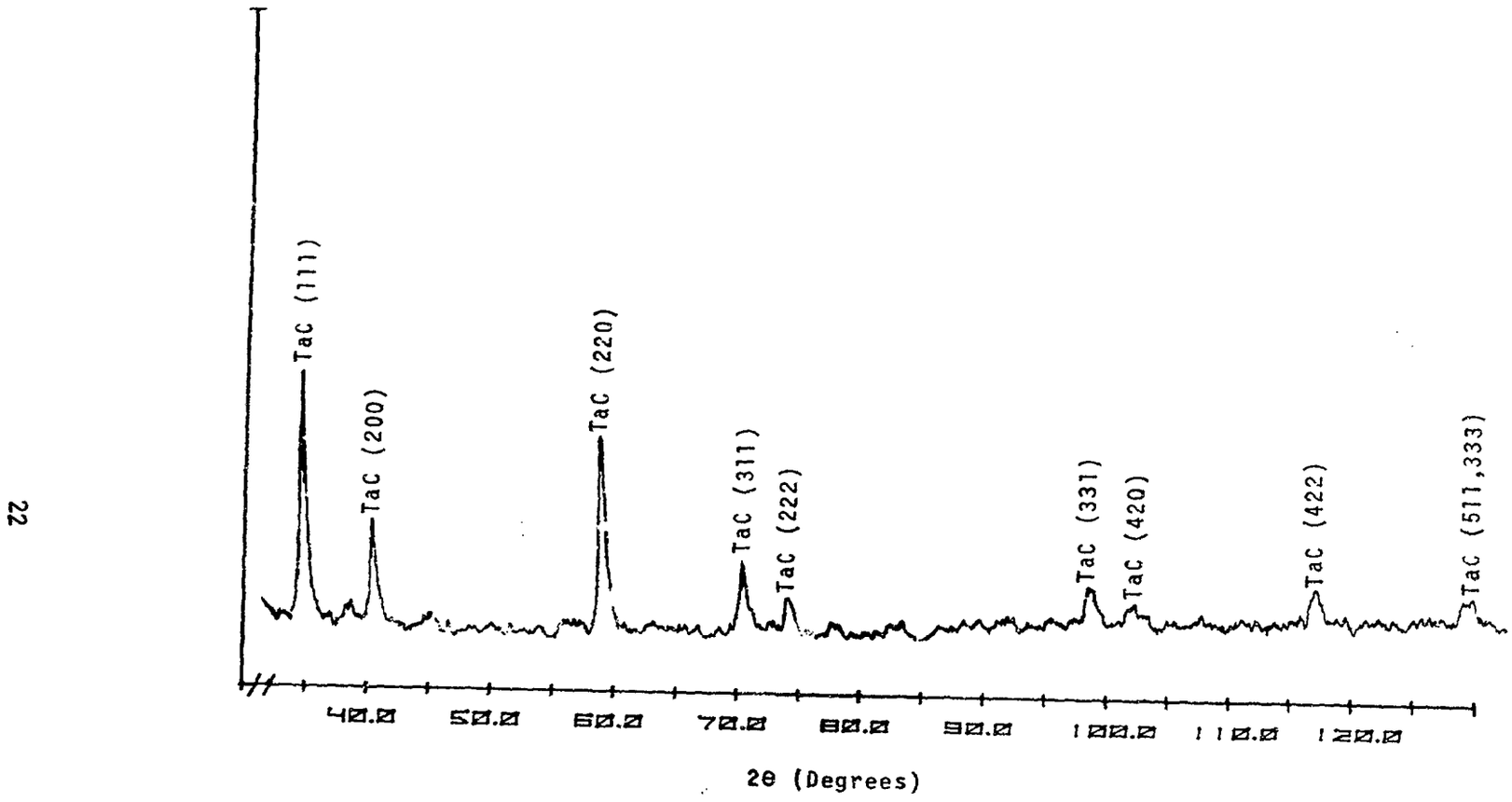

FIGURE 23. X-Ray Diffraction Pattern B.

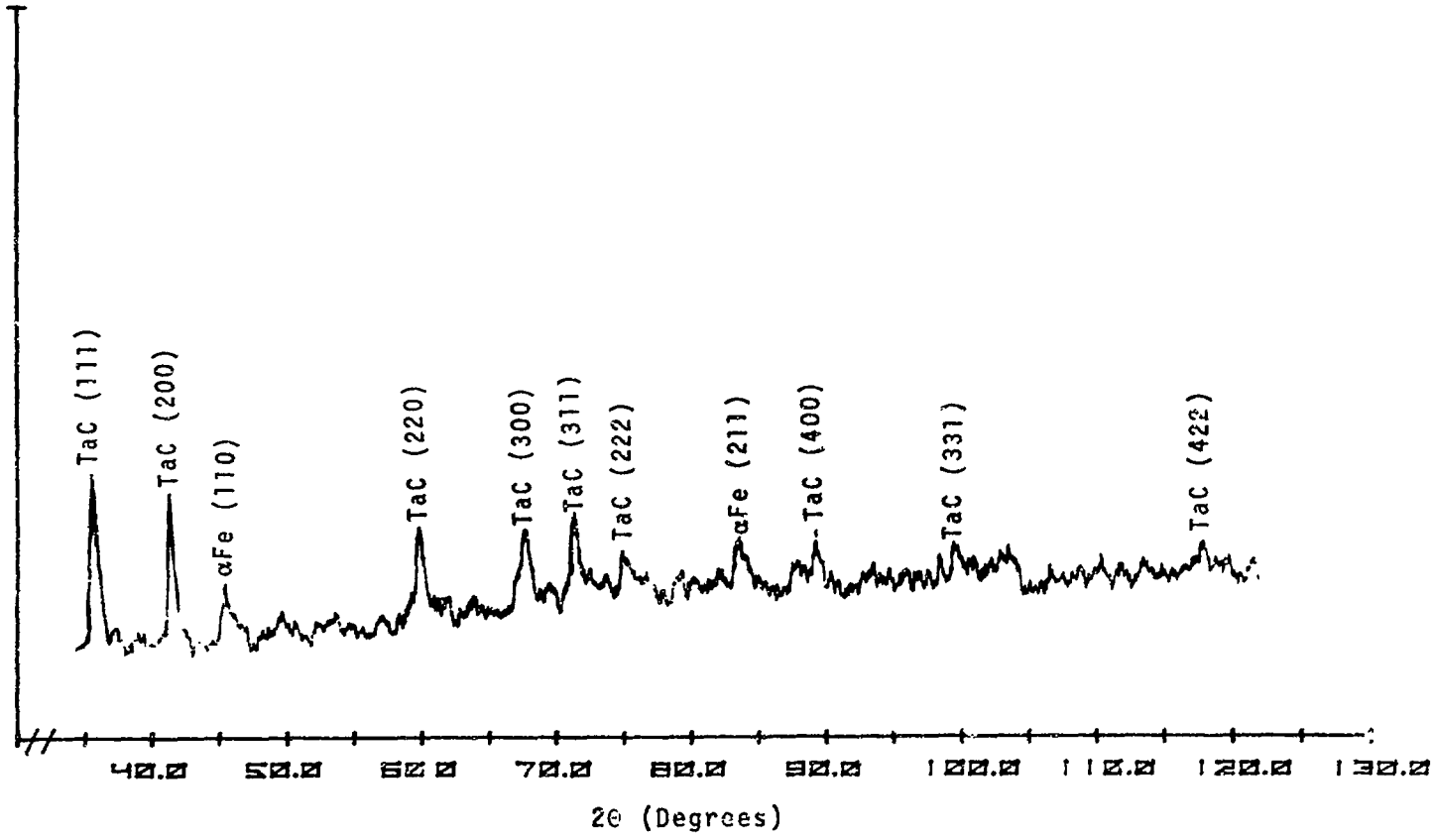

FIGURE 24. X-Ray Diffraction Pattern C.

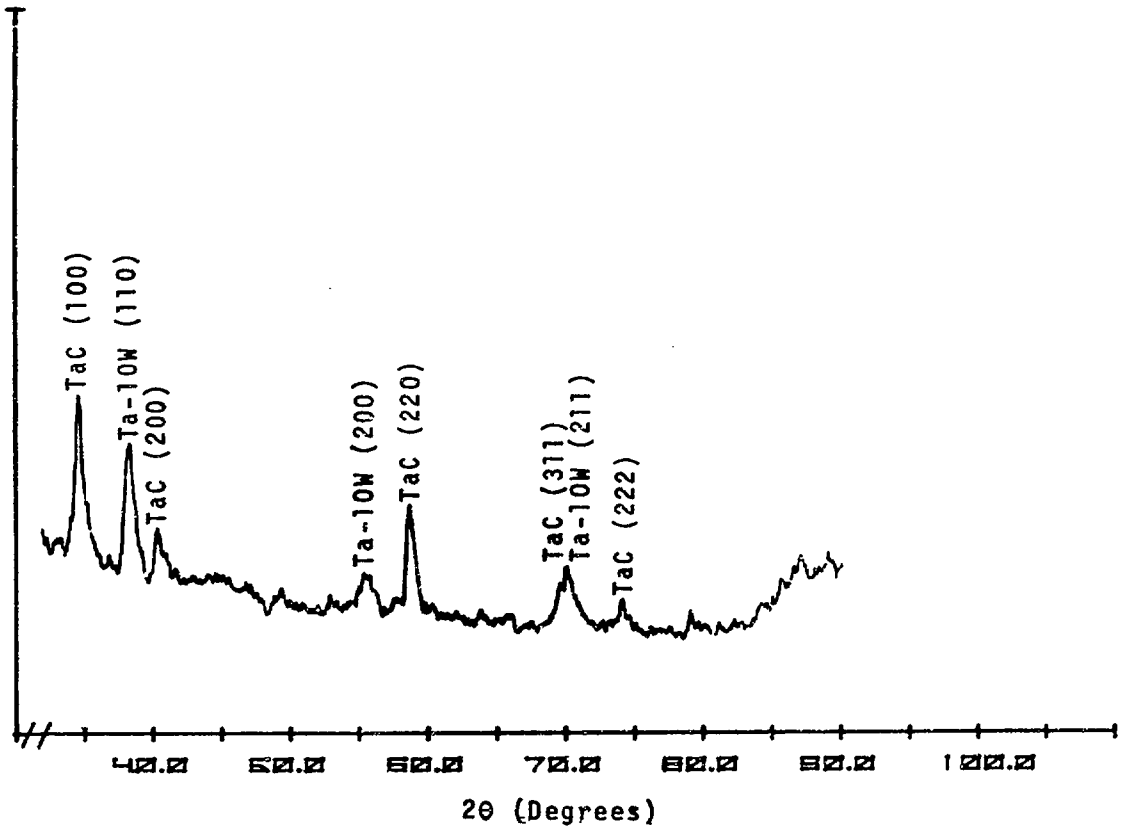

FIGURE 25. X-Ray Diffraction Pattern D.

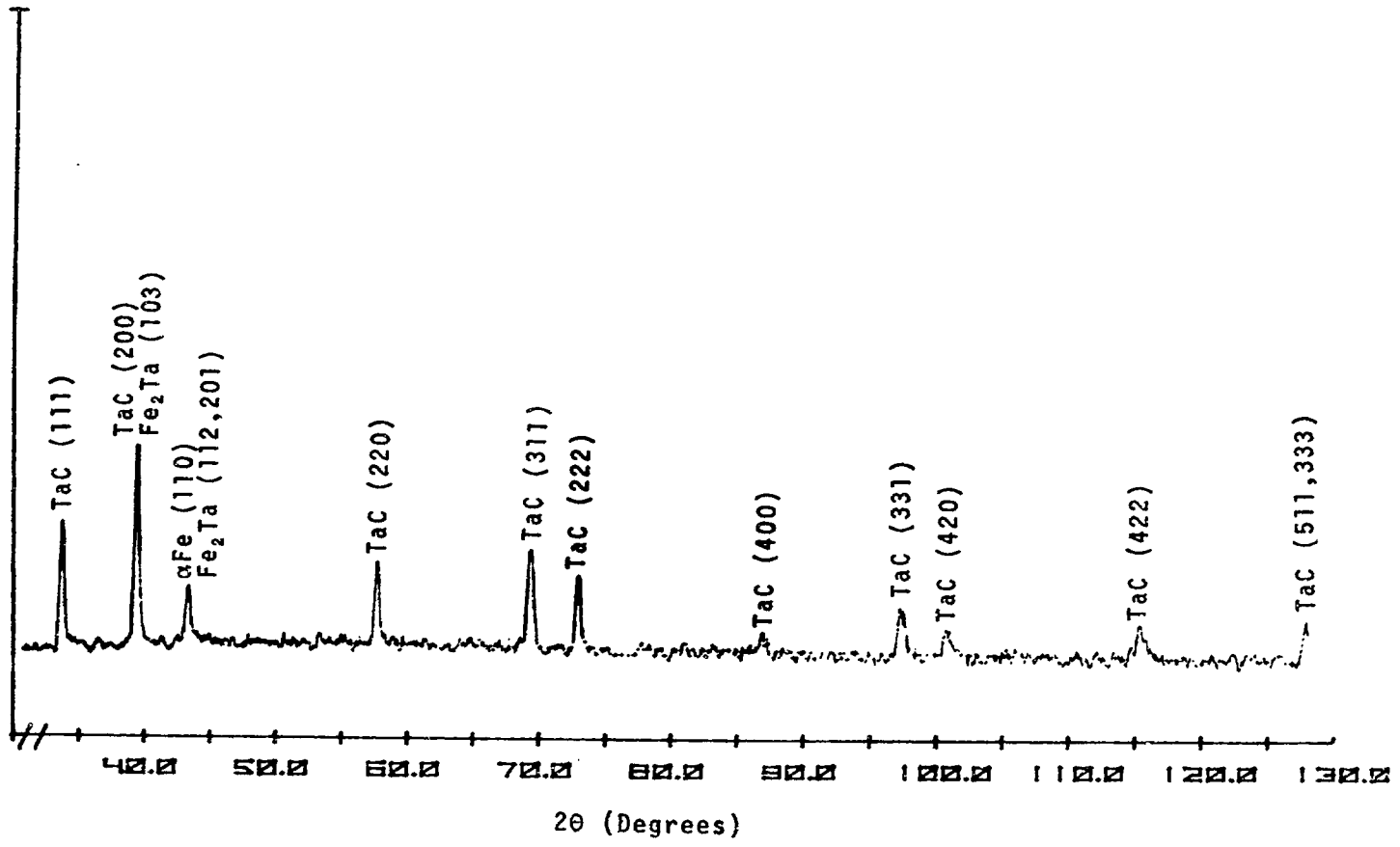

FIGURE 26. X-Ray Diffraction Pattern E.

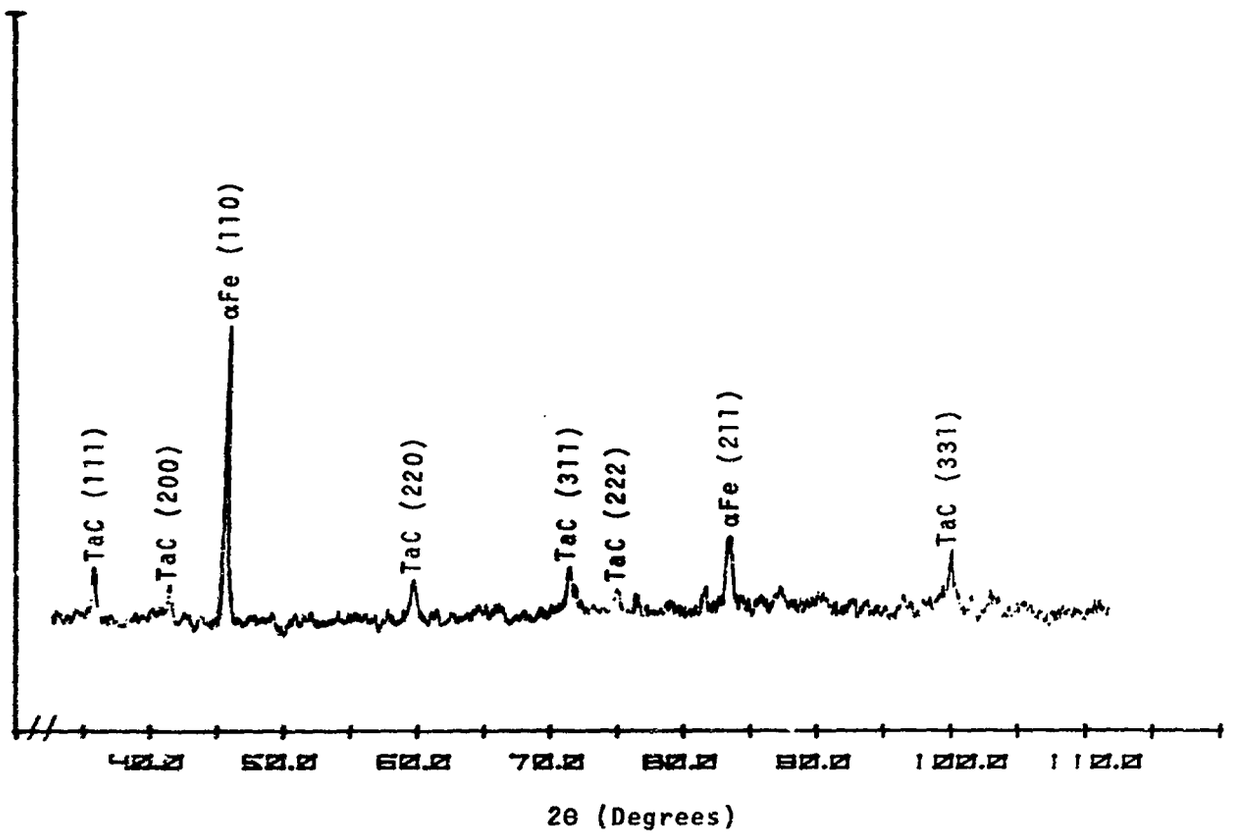

FIGURE 27. X-Ray Diffraction Pattern F.

FIGURE 28. Pattern G (left) and Pattern H (right) of Powder Specimens by Debye-Scherrer Technique.

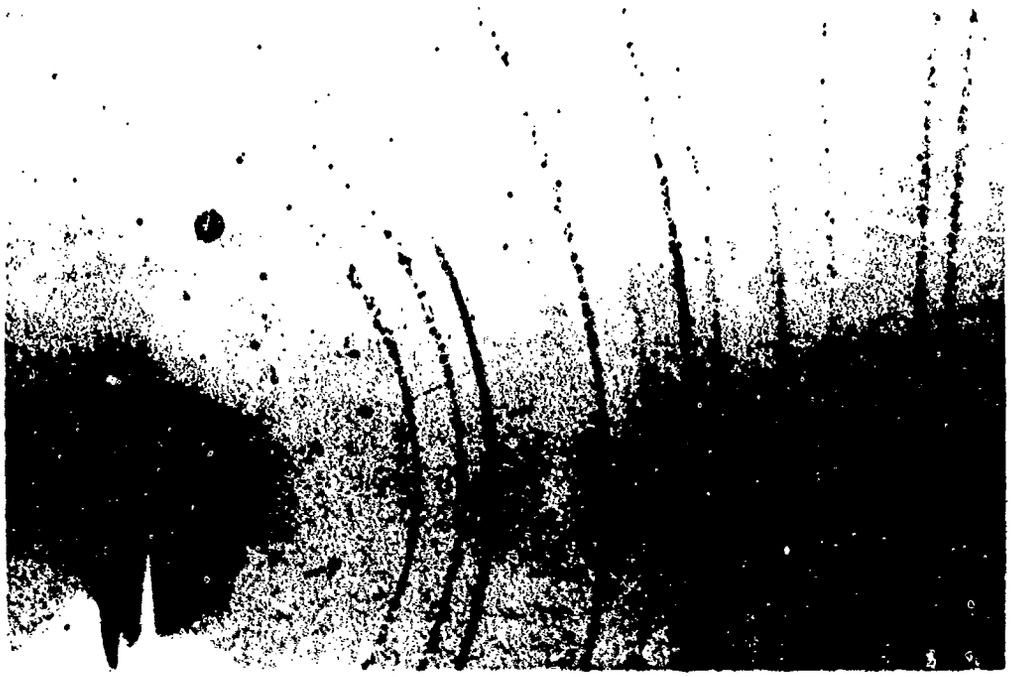

Line	d(A) - Measured	Index
1	2.63	2.57 - TaC (111)
2	2.23	2.23 - TaC (200)
3	2.05	2.03 - αFe (110)
4	1.57	1.57 - TaC (220)
5	1.45	1.43 - αFe (200)
6	1.33	1.35 - TaC (311)
7	1.27	1.29 - TaC (222)
8	1.17	1.17 - αFe (211)
9	1.10	1.12 - TaC (400)
10	1.015	1.02 - TaC (331)
11	.988	.996 - TaC (420)

FIGURE 29. Back Reflection Technique - Pattern I.

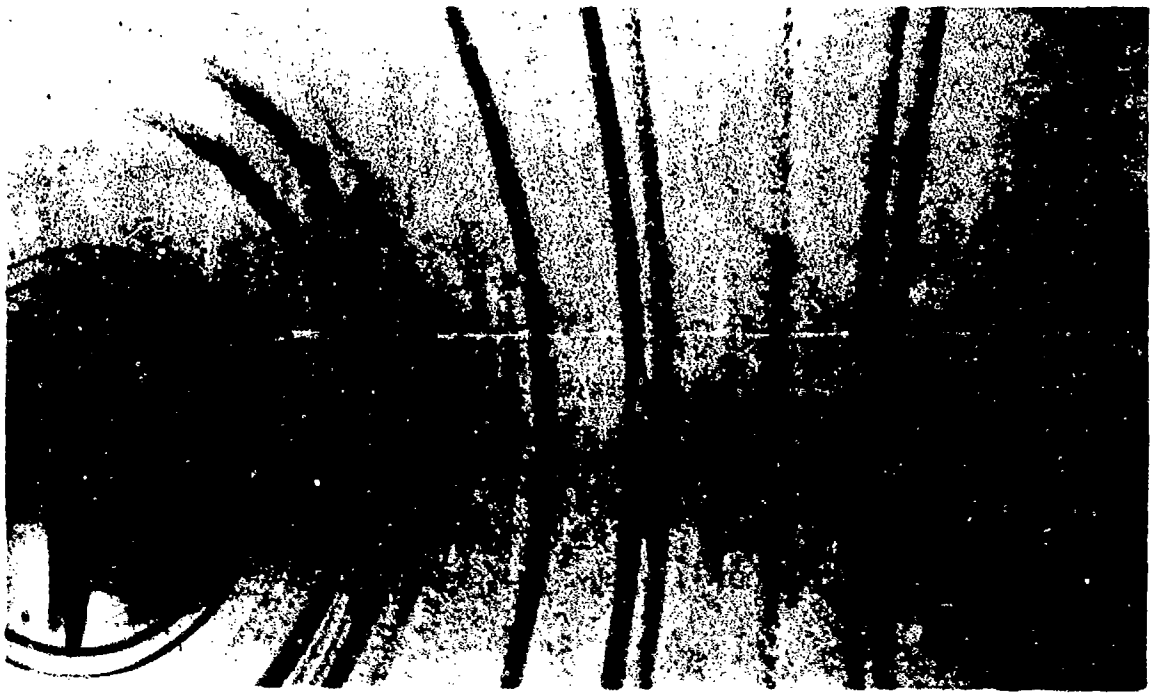

Line	d(A) - Measured	Index
1	4.11	4.15 - Fe_2Ta (100)
2	3.66	3.68 - Fe_2Ta (101)
3	2.49	2.57 - TaC (111)
4	2.20	2.23 - TaC (200) 2.22 - Fe_2Ta (103)
5	2.00	2.05 - Fe_2Ta (112) 2.02 - Fe_2Ta (201)
6	1.53	1.57 - TaC (220)
7	1.32	1.35 - TaC (311) Fe_2Ta (213)
8	1.27	1.29 - TaC (222)
9	1.09	1.12 - TaC (400)
10	1.01	1.02 - TaC (331)
11	.990	.996 - TaC (420)

FIGURE 30. Back Reflection Technique - Pattern J.

TABLE IV

COMPARISON OF PATTERNS G AND H WITH REFERENCE X-RAY DATA

Line	Intensity	d(Å)	Line	Intensity	d(Å)	TaC			αFe			Fe_2Ta			Ta-10W		
Pattern G			Pattern H			d	I/I₁	hkl	d	I/I₁	hkl	d	I/I₁	hkl	d	I/I₁	hkl
1.	MW	4.15										4.15	10	100			
												3.91	10	002			
												3.68	10	101			
2.	VVW	3.35															
3.	VW	3.14															
4.	S	2.84	1.	M	2.85							2.85	20	102			
5.	M	2.55	2.	VS	2.57	2.57	100	111				2.40	70	110	2.34	100	110
6.	M	2.22	3.	S	2.22	2.23	90	200				2.22	100	103			
			4.	M	2.06												
		(Split)										2.08	10	200			
7.	M	2.03	5.	M	2.02				2.03	100	110	2.05	100	112			
												2.02	70	201			
8.	W	1.64	6.	VW	1.63										1.65	21	200
9.	MW	1.57	7.	MS	1.57	1.575	75	220				1.95	5	004			
10.	VVW	1.40							1.43	19	200	1.39	20	300			
11.	M	1.33	8.	MS	1.35	1.349	55	311				1.35	40	213	1.35	38	211
12.	VW	1.28	9.	W	1.28	1.285	10	222				1.31	30	006, 302			
13.	VW	1.26	10.	VW	1.26							1.25	30	205, 106			
			11.	VVW	1.17				1.17	30	211				1.17	20	310
14.	VVW	1.15	12.	VVW	1.15												
15.	VVW	1.108	13.	VW	1.109	1.116	15	400									
16.	M	1.015	14.	M	1.018	1.022	30	331	1.013	9	220						
17.	M	.890	15.	M	.896	.896	30	420									

of diffusion with supplementary formation of the intermetallic Fe_2Ta. Carbon supplied by diffusion to form TaC results in a carbon-depleted zone in the steel.

The white zone exhibited in Figures 3 through 8 has been identified as TaC. The parabolic growth of the TaC observed in the samples heated at 2000°F is in agreement with that reported by Krikorian et al.[5] for surface carburization of tantalum although the growth rate constant differed by two orders of magnitude. This difference can easily be ascribed to variations in conditions.

Zone 1 of Specimen 5 and the matrix of Zone 2 are composed of TaC. Metallographic results (Figure 17) were the opposite of this conclusion and require further comment. The nitric and hydrofluoric acid mixture is known to dissolve tantalum carbides.[6,7] Zone 1 and the network extending into the Ta-10W alloy have been attacked by these acids. However, Zone 2 shows resistance to this etchant. This behavior was a result of a thought-provoking situation because, after the steel and the Fe rich Zone 3 had been chemically stripped from the sample in boiling HCl, Zone 2 was attacked by the HNO_3 plus HF similarly to Zone 1. The explanation involves the presence of two galvanic cells during etching. Zone 1 is anodic with respect to the Ta-10W and corrodes, but Zone 2 is cathodic to its Fe rich neighbor material and is protected from the acids.

The hardness of TaC has been recorded[7] as ranging from KHN 1800 to KHN 2000. The values determined in this investigation (Figures 18 and 19) are in fair agreement with this range when the possible sources of error, inherent in microhardness measurements with light loads, are considered.

Further evidence for the abundance of TaC was accumulated by observation of the diffusion Zones of Specimens 4 and 5 at low magnification. These zones exhibited a gold luster which is characteristic of TaC[7].

An explanation of the results is less distinct than the evidence. Diffusion couples in multicomponent systems offer extreme analytical complexity. Phase diagrams for systems such as the one in this investigation do not exist and, if they were available, only dubious prediction of the phases developed by diffusion could be accomplished because of the uncertainty of the diffusion path. The problem is thus reduced to one of speculation with only subsidiary binary phase diagrams for guidance. Three binary systems will be incorporated into the following discussion and essential neglect of the alloying elements in the steel

will be realized. Diffusion at the higher temperature, 2400°F (1315°C), could result in different phases than at 2000°F (1092°C). However, the binary diagrams of C-Ta, Fe-Ta, and Fe-W provide no basis for the occurrence of major variations. Therefore, sustained diffusion at lower temperatures can be considered to result in a diffusion zone comparable to that of Specimen 5.

The carbon-tantalum[8] system shows two carbides, Ta_2C and TaC. Since only TaC was detected in this study, the assumption is that either the Ta_2C phase is suppressed in the multicomponent or the more stable TaC is favored in the absence of complete equilibrium. Taking the composition of the TaC as approximately 6 weight per cent explains the ambient value of the Ta (80 weight per cent) in Zones 1 and 2 (Figure 21).

The iron-tantalum binary[8] contains one intermetallic-Fe_2Ta. This was identified by X-ray diffraction of Specimen 5. Metallographic study showed particles in Zone 2 and microprobe analysis indicated high Fe particles (in Zone 2) with an estimated composition of 35 to 40 weight per cent Fe, which agrees with the composition of Fe_2Ta in the binary system. The Fe_2Ta apparently occurs as discrete particles dispersed in TaC. This would explain the sporadic detection of Fe_2Ta by X-ray diffraction. The removal of fragments from the fracture surface (reference Pattern J, Figure 30) probably gave more favorable exposure of the Fe_2Ta particles to the impingent X-ray beam. This does not imply that the Fe_2Ta is concentrated in a zone below the TaC which would be contradictory to other results.

Tungsten diffusion into the steel was significant. Iron can accommodate appreciable amounts of tungsten in solution as exhibited in the Fe-W binary diagram.[8] The maximum solubility of tungsten in the ferrite was 5 weight per cent (Figures 20 and 21). Zone 3 probably accepted sufficient tungsten at the diffusion temperature to place the composition of this zone outside the gamma loop thereby eliminating the γ-α transformation on cooling. The coarse grains of Zone 3 would not be characteristic of a transformation product. The expected absence of a transformation implies that the carbon content of this zone is extremely low. Cooling of the solid solution α would be accompanied by rejection of the intermetallic WFe_2 (or more likely a complex intermetallic) due to the decrease in solid solubility of W in the α phase. This could well be the precipitate in Zone 3 (Figure 13).

Tantalum does not diffuse beyond the original interface, apparently as a consequence of the formation of TaC. The "high-tungsten" particles found in Zone 2 are probably tungsten carbides or complex carbides. Tantalum and tungsten form a complete series of solid solutions ruling out the possibility for an intermetallic.

A review of this investigation will be helpful in relating the results to the events that occur in a gun barrel operating at elevated temperatures. Carbon diffuses from the steel and combines with the Ta-10W alloy, thus TaC and scattered tungsten carbides are formed and the steel at the diffusion interface is depleted of carbon. Simultaneously, tungsten diffuses into the steel forming a solid solution and iron diffuses into the Ta-10W forming discrete particles of the intermetallic Fe_2Ta which end up dispersed in a matrix of TaC. The TaC is the predominant diffusion product and is a hard brittle constituent. Note that separation of the liner from the steel was accomplished without difficulty by fracturing through the diffusion zone.

The diffusion zone of Specimen 5 should not be construed to represent the actual diffusion zone in a gun barrel because the quantity of diffusion necessary to develop such a zone would not be expected to occur during manufacturing or the firing of a gun barrel. However, note that the diffusion process described in the previous paragraph will be operative on a smaller scale in the barrel and that the diffusion zone formed will continually approach that of Specimen 5, being limited only by the dependence of diffusion on time and temperature.

CONCLUSIONS

1. Tantalum carbide (TaC) is the predominant phase formed by diffusion between Ta-10W and 4150 steel.

2. Growth of the TaC obeys a parabolic rate law and grows in the direction of the Ta-10W.

3. The diffusion zone is hard and brittle, and is easily fractured resulting in separation of liner and steel.

4. The intermetallic Fe_2Ta forms as particles in a matrix of TaC.

5. Carbon diffusion results in a carbon depleted zone in the steel adjacent to the original interface.

6. The extent of tungsten diffusion into the steel is appreciable.

7. Tantalum does not diffuse into the steel to any appreciable extent.

8. Particles of high-tungsten concentration, probably tungsten carbides, are present in the TaC matrix.

9. Three distinct zones are formed by diffusion. The zones are identified as:

Zone 1 - TaC

Zone 2 - TaC with Fe_2Ta and high-tungsten particles and

Zone 3 - Carbon-depleted steel with tungsten in solid solution.

10. The diffusion times and temperatures, necessary to enlarge the diffusion zone to a critical thickness whereby fracture of the multilayer gun barrel could occur, are not attainable in gun barrel environments.

LITERATURE CITED

1. DiBenedetto, J. D., "Multilayer Gun Barrels for Rapid-Fire Weapons," R&E Directorate, U. S. Army Weapons Command, Report RE-TR-70-195, 1970.

2. Forgeng, W. D., Chapter 9 of Columbium and Tantalum (Sisco and Epremian editors), John Wiley and Sons, New York, 1963.

3. Dillinger, L., DMIC, Battelle Memorial Institute, private communication.

4. Wallbaum, H. J., Z. Krist., 103, 1941, 391-402.

5. Krikorian, N. H., T. C. Wallace, R. Krohn, and M. G. Bowman, Los Alamos Scientific Laboratory Report LADC 8803, "The Formation of Carbide Surfaces on Tantalum," 1967.

6. Ellinger, F. H., "Trans. ASM," 31, 1943, 89-104.

7. Shelpline, V. H., and R. J. Runck, Chapter 5 of High Temperature Technology," (edited by Campbell), John Wiley and Sons, New York, 1956.

8. Hansen, M., Constitution of Binary Alloys, McGraw-Hill, New York, 1958, p. 381-721.